

Numerical Study of Fatigue Behaviour for AA6082-T6 Aluminium Alloy Friction Stir Welds under Monotonic and Variable Amplitude Loading

Y. Kambouz, M. Benguediab, B. Bouchouicha and M. Mazari

University of SidiBel-Abbes-ALGERIA, Materials and Reactive Systems Laboratory

Abstract: In addition to uncertainty such as material strength, notch geometries, defect contents and residual stresses, welded components are often subjected to variable amplitude service loads. The objective of this investigation is to determine the fatigue strength of friction stir welds in AA6082-T6 under constant and variable amplitude loading and analyse the validity of Miner's rule in this specific welding process. Microhardness tests were performed to characterize the Vickers hardness profile in the vicinity of the weld area. Friction stir welding process leads to a decrease of the static mechanical properties relatively to base material. Detailed examination revealed a hardness decrease in the thermo mechanically affected zone and the nugget zone average hardness was found to be significantly lower than the base alloy hardness. Welded specimens show significantly lower lives than base material specimens.

Key words: Friction Stir Welding • Aluminium alloy • Fatigue • Variable amplitude loading

INTRODUCTION

Friction stir welding (FSW) is a relatively new solid-state joining process and is very energy efficient, environment friendly and versatile, being considered to be the most significant development in metal joining in a decade. Since its invention in 1991 at the Welding Institute (TWI) of UK [1], a large amount of research was carried out in several fields and different materials

Aluminium alloys are the materials more often studied and where this technique has shown a better performance. Comparative mechanical properties studies of base material and welded specimens, including fatigue strength tests have been performed by several authors [2-6].

In addition to uncertainty such as material strength, notch geometries, defect contents and residual stresses, welded components are often subjected to variable amplitude service loads. The lack of Miner's validity accumulation rule [7] has been demonstrated in many applications and, in consequence, its usage will introduce uncertainties which must be compensated by safety factors. In the case of friction stir welding (FSW) no data is available concerning fatigue behaviour under variable amplitude loading.

The objective of this work is to study the fatigue strength of friction stir welds under constant and variable amplitude loading and analyse the validity of Miner's rule for this specific welding process.

Presentation of the Material: The material used is an aluminum alloy 6000 series subjected to T6 treatment, which will help the investigation of the various phenomena that occur during welding with involving the precipitation phenomenon.

This aluminum alloy is a high strength Al-Mg-Si alloy that contains manganese to increase ductility and toughness. The T6 condition is obtained through artificial ageing at a temperature of approximately 180°C [8].

Hardness Profile and Mechanical Properties of the Material: The most commonly used practice is the measurement of microhardness which gives a first evaluation of the mechanical properties in different areas of the weld, in order to obtain a profile across it and to establish the weld zones. It is a direct result of the change in the microstructure caused by the welding process.

The optimization of the weld process FSW requires the mechanical characterization of the weld bead.

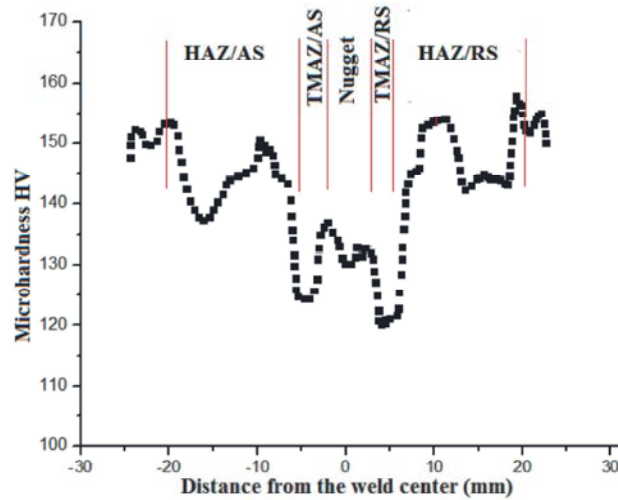


Fig. 1: Hardness profile

The Pictures of the microstructure of the different areas of the AA6082-T6 alloy aluminum can be found in [9]. The Vickers hardness profiles for all areas (BM, HAZ, TMAZ and nugget) are presented in Fig. 1. A hardness decrease occurs when approaching the TMAZ. The average hardness of the nugget zone was found to be significantly (lower than the hardness of the base Metal). There is a zone outside the nugget (transition between TMAZ and HAZ) which has the lower hardness value. In Svensson LE, Karlsson L, Larsson H [10] it is suggested that the variation of the microhardness values in the welded area and parent material is due to the difference between the microstructures of the base alloy and weld zone.

In the tensile tests of the dissimilar specimens it was observed that the fracture surface is coincident with this zone of lower values of hardness.

The monotonic tensile tests were performed to determine the mechanical properties of the welded and unwelded materials: the yield stress R_e , the rupture stress R_m , the Young modulus E and the elongation $A\%$. The mechanical properties are given in Table 1.

This table shows the mechanical properties of welded specimens obtained in tension tests, compared with base material.

The friction stir welding process leads to a decrease of the material mechanical properties: yield and rupture stresses of friction welded specimens are significantly lower than for base material.

Lifetimes of Fatigue and Damage in the Zones of Welding: To determine the distributions of stress, strain and tensile strength of the aluminum alloy 6082-T6 no

welded and welded the ANSYS software was used. This calculation code is based on the Finite Element method designed for the analysis of structures. It can treat problems of linear elasticity and nonlinear (élastovisco plastic), dynamic problems transient and steady, transient and stationary thermal problems.

It is necessary to add that a program "DELPHI" was used to import the input data such as constraints and numbers of cycles applied to the specimens used for the simulation of fatigue behavior.

Local Fatigue Behavior: The specimen used is a CT-50 according to ASTM-E-647. Figure 2 shows a welded and non-welded specimen. The mesh size used is refined near the crack tip. The crack tip is indicated by the ratio of two geometric sizes a_0 and W .

The fatigue results obtained for the stress ratio $R=0.1$, under constant amplitude loadings are plotted in Figures 4.

These curves are used to estimate the lifetime of the structure and to determine the reduction in life of FSW welds compared to the base material.

Due microstructural heterogeneities, the FSW welds have very heterogeneous mechanical behavior. In each of the zones of welding (HAZ, ZATM and Nugget). The friction stir welded AA6082-T6 specimens presented significantly lower lives than base material specimens. In practice this reduction may vary depending on the load applied, the surface state and weld defects.

In this study the weld seams were considered without defects. The results of the analysis are summarized in Table 2.

Table 1: Mechanical properties of aluminum alloy 6082-T6

Nuance	Metallurgic state	R _p [MPa]	R _m [MPa]	A%	E [MPa]
6082 supplier	T6	310	350	12	69000
6082	T6	265	321	10.5	68000
6082 (FSW)	T6	135.8	220.5	7.5	51200

Table 2: Results of Fatigue endurance for base metal and welded bead

N°	σ_{max}	σ_{min}	σ_m	Cycles to Failure (N _f)			
				Base metal	Nugget	TMAZ	HAZ
1	275	27.5	151.25	68967	59344	49635	38520
2	260	26	143	131607	98400	67865	51535
3	250	25	137.5	205541	156587	99810	73401
4	240	24	140	380805	255500	162599	116910
5	230	23	126.5	650125	438000	280050	186760
6	225	22.5	123.75	875010	568997	385000	240500
7	200	20	110	3150000	2090000	1403020	1001000

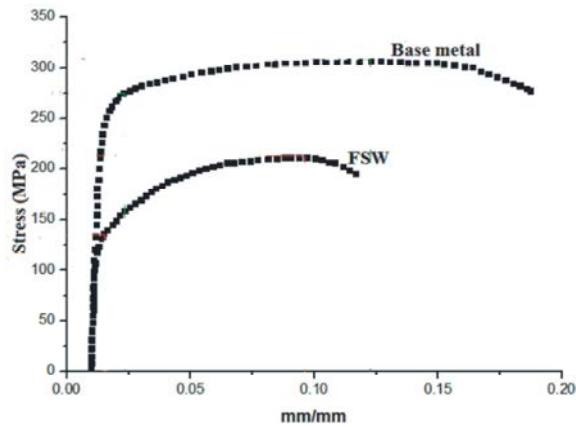


Fig. 2: Tensile tests

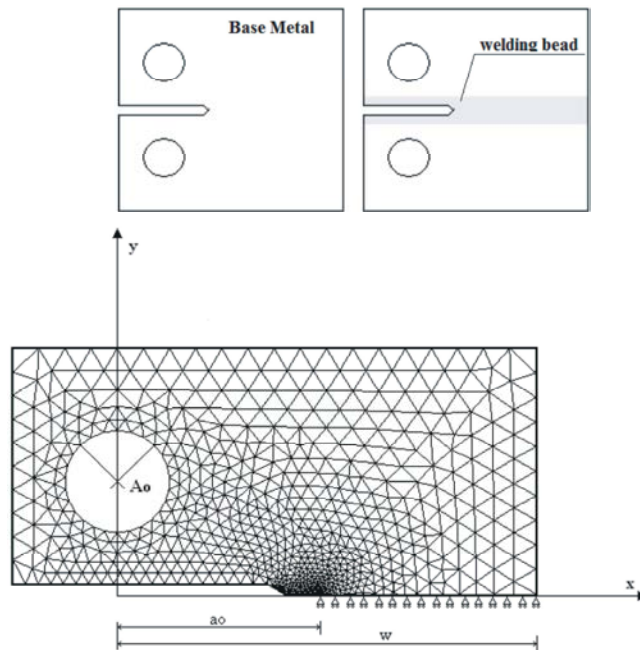


Fig. 3: CT-50 specimen welded and non-welded

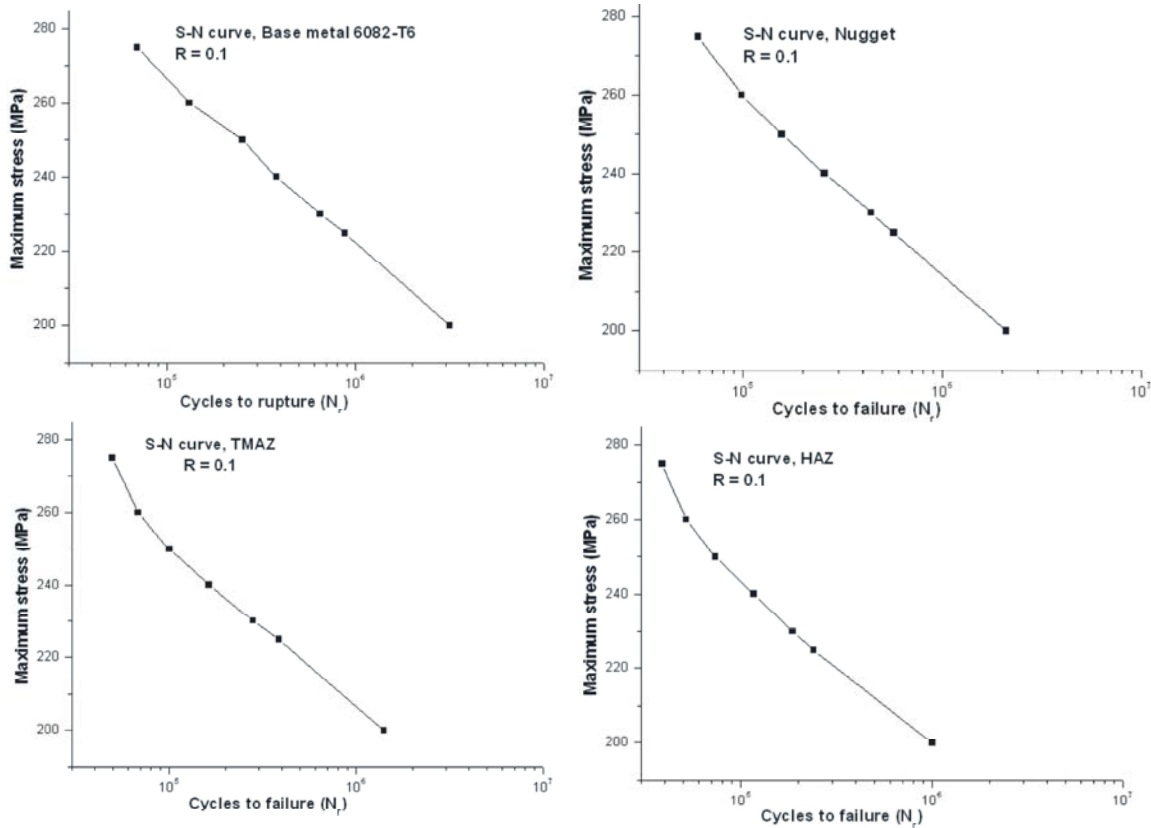


Fig. 4: Fatigue endurance curves of the base metal and welded joint

Table 2 shows that the weld zone has a low fatigue resistance compared to the base material.

The fatigue strength of the welded joint is not primarily governed by the resistance of the base metal. The most important parameters are global and local geometry of the welded joint.

Lifetimes of Fatigue: The study of the lifetimes was made by using ANSYS with a sub program "DELPHI" Fatigue simulations were performed under ANSYS under sinusoidal loading imposed with a ratio of $R = 0.1$ (Figure 4).

The results obtained for the various tests on CT-50 mechanical test pieces having a notch through the thickness of the sheet and located in the four areas (BM - Nugget - TMAZ and HAZ) are shown in Figure 4 and Figure 5. At the same level of ΔK , generally there is a crack propagation rate da / Dn , lower in the BM to that of the nugget which is less than that of TMAZ and HAZ [12]. However, the difference between these speeds decreases when ΔK increases Figure 7. This phenomenon is encountered in the case of 2024-T235 aluminum alloy

and 6061-T6 [12-14]. For both types of aluminum this speed reduction is generally accompanied by the crack deviation from its initial plan to the HAZ. Some authors [14-15] have attempted to explain this deviation by the difference in mechanical properties between the four areas. The crack from a harder microstructure, to a soft microstructure.

Cumulative Damage: To quantify the pre-encumbrance it shows that it is permissible to take the model Palmgren-Miner [7].

It then establishes the damage as a fraction of the total life.

Two levels of maximum stress were selected; 200 and 275 MPa corresponding to numbers of cycles to failure N_f (100% damage: $D = 1$).

The results are shown in Table 3, 4 and 5.

The three modes of loading clearly show a low resistance to fatigue in the welding area. Particularly in the HAZ or there has been a significant decrease in fatigue life.

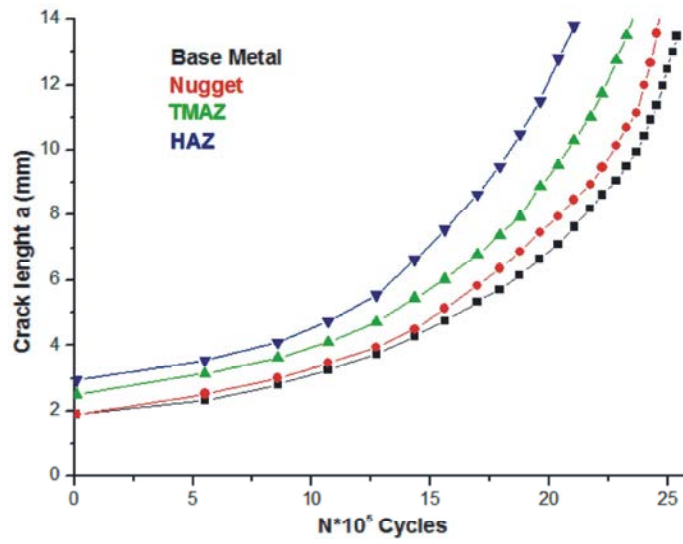


Fig. 5: Crack propagation based on the number of cycles

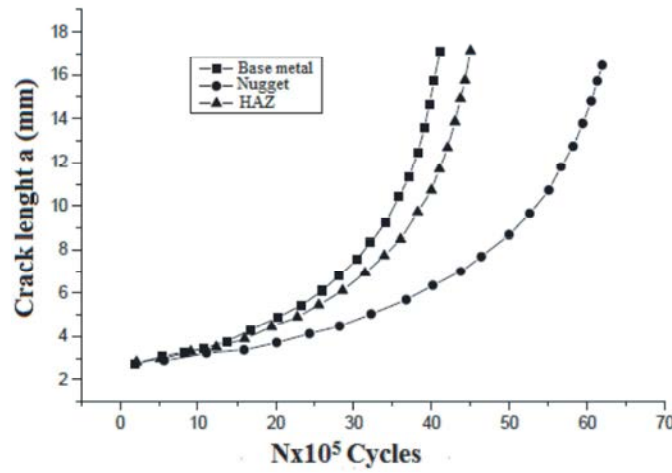


Fig. 6: Crack propagation based on the number of cycles [11]

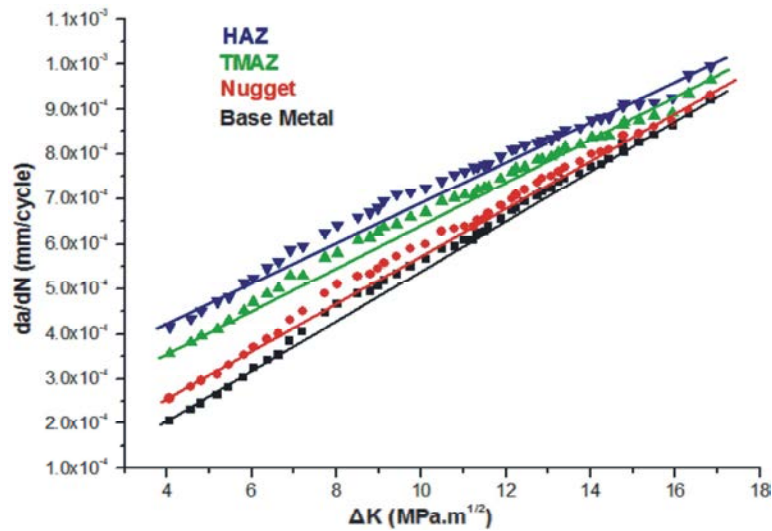


Fig. 7: Cracking speed according to ΔK

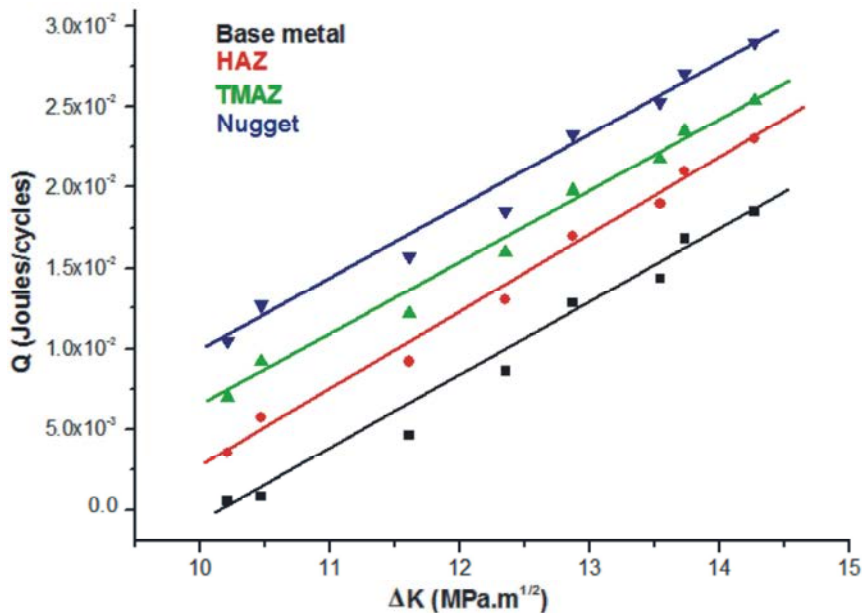


Fig. 8: Evolution of hysteretic energy based ΔK

Table 3: Loading down/up in different welding zones

Loading down / up				
$\sigma_2 = 275$ MPa				
n* (Number of remaining cycles)				
$\sigma_1 = 200$ MPa	BM	Nugget	TMAZ	HAZ
$n_1 = 500000$	58188.01	45146.97	31946.12	19279.27

Table 4: Loading up/down in different welding zones

Loading up / down				
$\sigma_2 = 200$ MPa				
n* (Number of remaining cycles)				
$\sigma_1 = 275$ MPa	BM	Nugget	TMAZ	HAZ
$n_1 = 25000$	2011451	1209584.02	696343.85	351338.33

Table 5: Random Loading in different welding zones

Random loading					
$\sigma_3 = 275$ MPa					
n* (Number of remaining cycles)					
$\sigma_1 = 250$ MPa	$\sigma_2 = 200$ MPa	BM	Nugget	TMAZ	HAZ
$n_1 = 40000$	$n_2 = 500000$	44730	30029	12111	Failure

Evolution of Energy Q Based on ΔK : Figure 8 shows the evolution of the energy dissipated hysteretic Q for a cycle based ΔK for a load ratio $R = 0.1$ in the four areas studied (BM –Nugget -TMAZ - HAZ). This energy is determined by a numerical integration of cycles (Δ -P), its expression is obtained by calculating the area of the loop obtained by

acquisition and processing by a program written in LABVIEW. The advantage of this program is to be able to estimate this hysteretic energy for low values of ΔK . We note that Q increases when ΔK increases for the four study areas.

Residual Stresses

Terms of Simulation: During charging, there is stress concentration around Nugget because of their Young's modulus different from that of the TMAZ. The highest stresses that develop near the Nugget, it promotes localized plastic deformation. When a fatigue crack propagates in a medium loaded in the elastic field creates a plasticized region at its tip that induces a residual compressive stress field in Figure 9. In the case of a repeated loading or corrugated this field of constraints to the tip of the crack leads to a partial closure thereof during a part of the loading cycle [16].

To generate a residual stress field in elastic-plastic behavior, the applied stress must exceed the elastic limit.

Therefore, we use a loading rate σ_{App} / σ_e equal to 1.05 in the ABAQUS code, making loads at room temperature of 25 °C.

The residual stresses at the crack tip, are compressive nature with decreasing absolute values depending on the length of the crack.

Figure 9 shows the evolution of the residual stress at a loading rate of 1.05 at room temperature of 25°C. Note that the tip of the crack residual stresses are compressive stresses that evolve with the evolution of the crack.

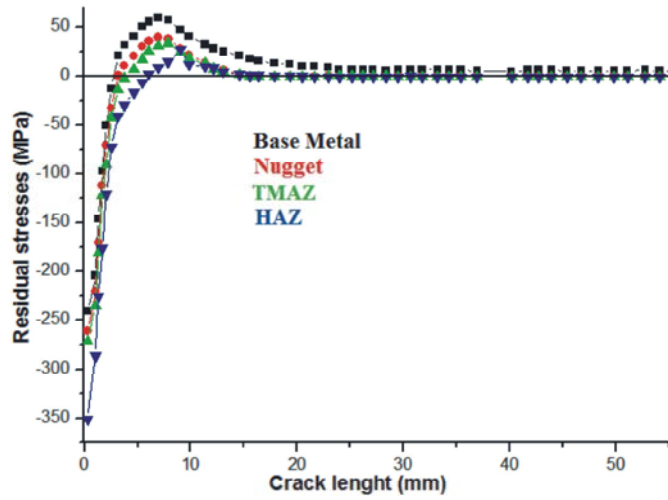


Fig. 9: Residual stresses as a function of the propagation of the crack

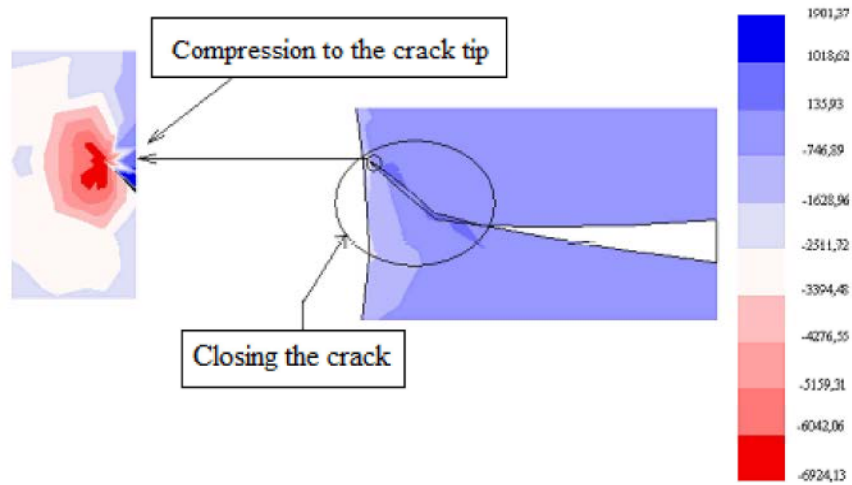


Fig. 10: Close to the crack tip [18]

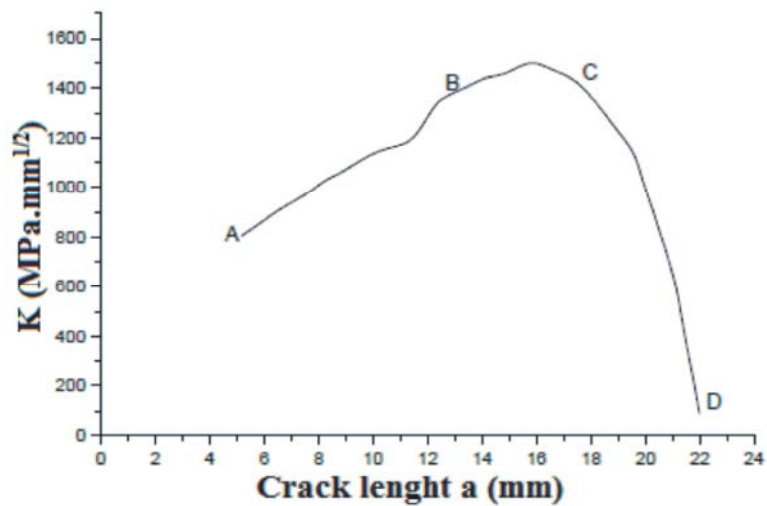


Fig. 11: Variation of K_I depending on the length of the crack [18]

For each advance of the crack, the residual stresses pass through a compression phase and a voltage phase away from the crack tip these stresses tend to zero, so there is stress relaxation [17].

Figure 11 shows the variation of the stress intensity factor based on the length of the crack.

It is noted in this figure that there are three stages, AB BC and CD. The crack is fully open between AB relationship is growing and gradually closes between BC and CD is closed between the relationship is decreasing.

This configuration change is explained by the phenomenon of closure. Elber [17] showed that a fatigue crack can be closed even when the structure is further subjected to a tensile

Compressive stresses are created around the crack when the load tends to zero. He concluded that a fatigue crack differs from a perfect mechanical crack because it creates a residual deformation zone during propagation

The theoretical opening of the tip of the CTOD crack is thus reduced. Assuming that a fatigue crack does not spread when closed, he concludes that it is wrong to consider the total amplitude of the cycle to establish the relationship of Paris and proposes to replace the factor stress intensity of this relationship through effective stress intensity factor $\Delta K_{eff} = K_{max} - K_{op}$ where K_{max} is the maximum stress intensity factor, K_{op} the stress intensity factor required to fully open the crack [18].

CONCLUSION

The analysis of welded structures does not deviate too much from that of other types of structures.

Due to the heterogeneity of microstructure present in FSW welds under quasi-static monotonic loading, we have a highly heterogeneous mechanical behavior in each of the areas (BM, HAZ, TMAZ and Nugget). To highlight these heterogeneities in the fatigue testing, the same approach developed in the case of quasi-static tests monotonous traction has been adapted.

The simulation results are presented in Tables 2, 3, 4 and 5 respectively for one block, two blocks (down / up), two blocks (up / down) and random. These results show that the fatigue strength of welded FSW joints is significantly lower. This result for the base material (MB) and the welded material, show a realistic simulation with ANSYS. This simulation gives the advantage to visualize damaged areas and allows manufacturers to optimize the lifetime of structures; to avoid significant damage and loss of life.

The fatigue crack initiation begins and grows in the vicinity of the weld during the service life. The fatigue strength of the welded joint is not primarily governed by the resistance of the base metal. The most important parameters are global and local geometry of the welded joint.

Several mechanisms have to be avoided in the appropriate design, the choice of metal and dimensions of structures.

The results of this study open interesting prospects for modeling the mechanical behavior of FSW joints and to assess their fatigue life.

When the Nugget is harder than the TMAZ ($E_{Nugget} / E_{TMAZ} = 2$), the maximum stresses are obtained at the Nugget. The presence of Young's modulus difference therefore weakens the structure and can increase the risk of cavities and priming germination microcracks.

REFERENCES

1. Thomas, W.M., E.D. Nicholas, Needham, J.C. Much, M.G.P. Temple Smith and C.J. Dawes, 1991. G.B. patent application No. 9125978.8.
2. Ericsson, M. and R. Sandstrom, 2003. Influence of welding speed on the fatigue of friction stir welds and comparison with MIG and TIG. *International Journal of Fatigue*, 25: 1379-1387.
3. Moreira, P.M.G.P., A.M.P. Jesus, A.S. Ribeiro and P.M.S.T. Castro, 2008. Fatigue crack growth in friction stir welds of 6082-T6 and 6061-T6 aluminium alloys: A comparison. *Theoretical and Applied Fracture Mechanics*, 50-2: 1-91.
4. Lanciotti, A. and F. Vitali, 2003. Characterisation of friction stir welded joints in aluminium alloy 6082-t6 plates. *Welding International*, 17-8: 624-630.
5. Kobayashi, Y., M. Sakuma, Y. Tanaka and K. Matsuoka, 2007. Fatigue Strength of Friction Stir Welding Joints of Aluminium Alloy 6082 Extruded Shape. *Welding International*, 21-1: 18-24.
6. Cavaliere, P., A. De Santis, F. Panella and A. Squillace, 2009. Effect of welding parameters on mechanical and microstructural properties of dissimilar AA6082-AA2024 joints produced by friction stir welding. *Materials and Design*, 30: 609-616.
7. Miner, M.A., 1945. Cumulative damage in fatigue, *J. Appl Mech.*, 12: 159-64.
8. Myhr, O.R. and Grong, 1991. Process modelling applied to 6082-T6 aluminium weldments-1 Reaction kinetics-2 Applications of the model, *Acta. metal. Mater.*, 39: 2693-2708.

9. Wan Long, Yongxian Huang and Weiqiang Guo, Mechanical Properties and Microstructure of 6082-T6 Aluminum Alloy Joints by Self-support Friction Stir Welding.
10. Svensson, L.E., L. Karlsson, H. Larsson, B. Karlsson, M. Fazzini and J. Karlsson, 2000. Microstructure and mechanical properties of friction stir welded aluminium alloys with special reference to AA 5083 and AA 6082. *Sci Technol Weld Joining*, 5: 285-96.
11. Ghazi, A., M. Mazari, A. Imad and B. Benamar, 2010. Modeling of the propagation of cracks in a welded structure, *Computational Materials Science*, 50: 633-638.
12. Lieurade, H.P., 1995. Application de la mécanique de la rupture à la fissuration par fatigue des composants soudés, Publication Cetim-admissibilité des défauts dans les structures.
13. Diez, J.M., 1972. ECSC Agreement, pp: 6210-28.
14. Kobayashi, H., 1980. *I. Mech. E.*, pp: 38-80.
15. Rabbe, 1979. I I W DOC XIII-914-79.
16. GHAZI, A., Caractérisation mécanique des assemblages soudés par friction malaxage, Thèse de Doctorat-Université de Sidi Bel-Abbes.
17. Elber, W., ASTM STP, 486-1971, 230-242.
18. Claud Bathias and J.P. Bailon, 1997. *La fatigue des matériaux et des structures*, Hermes.